UDC 621.3 **doi: 10.20998/2074-272X.2020.6.09**

R. Lebied, R. Lalalou, H. Benalla, K. Nebti, I. Boukhechem

AMELIORATE DIRECT POWER CONTROL OF STANDALONE WIND ENERGY GENERATION SYSTEM BASED ON PERMANENT MAGNET SYNCHRONOUS GENERATOR BY USING FUZZY LOGIC CONTROL

Purpose. Electricity is a basic energy for life and its consumption increased so we need the discovery of new sources of energy such as wind energy .for this ameliorate the quality of generated wind energy by using the intelligent artificial control, this control is made to optimize the performance of three-phase PWM rectifier working. Methodology. These strategies are based on the direct control of the instantaneous power, namely: the control direct power control (DPC) with classic PI regulator and direct power control with fuzzy logic regulator. The fuzzy characterized by its ability to deal with the imprecise, the uncertain has been exploited to construct a fuzzy voltage regulator. The simulation of these methods was implemented using Matlab/Simulink. Results. A comparison with the results obtained by the classic PI showed the improvement in dynamic performance. This makes the fuzzy controller an acceptable choice for systems requiring quick, precise adjustments and less sensitive to outside disturbances. Originality. The proposed this control strategy using for to obtain a performance adjustment of the DC bus voltage and sinusoidal currents on the network side. Practical value. Fuzzy logic is proven to be effective in terms of reducing the harmonic distortion rate of the currents absorbed, correct adjustment of the active and reactive power and DC voltage and unit power factor operation. References 26, tables 6, figures 15.

Key words: **direct power control, fuzzy logic control, permanent magnet synchronous generator (PMSG), PWM technique, wind energy system.**

Мета. Електроенергія є основною енергією для життя, і її споживання збільшується, тому нам необхідно відкриття нових джерел енергії, таких як енергія вітру. Для поліпшення якості енергії вітру, що генерується за допомогою управління на основі штучного інтелекту, таке управління призначене для оптимізації продуктивності роботи трифазного ШІМ випрямляча. Методологія. Дані стратегії засновані на прямому управлінні миттєвою потужністю, а саме: пряме управління потужністю з класичним ПІ-регулятором і пряме управління потужністю регулятором з нечіткою логікою. Нечіткість, що характеризується її здатністю справлятися з неточністю, невизначеністю, була використана для створення нечіткого регулятора напруги. Моделювання цих методів було реалізовано за допомогою Matlab/Simulink. Отримані результати. Порівняння з результатами, отриманими за допомогою класичного ПІ-регулятора, показало поліпшення динамічних характеристик. Це робить нечіткий контролер прийнятним вибором для систем, що вимагають швидкої і точної настройки і менш чутливих до зовнішніх перешкод. Оригінальність. Запропоновано стратегію управління, що використовує для отримання регулювання продуктивності напруги шини постійного струму і синусоїдальні струми на стороні мережі. Практична цінність. Доведено, що нечітка логіка ефективна з точки зору зниження коефіцієнта гармонійних спотворень поглинаються струмів, коректного регулювання активної і реактивної потужності і постійної напруги, а також коефіцієнта потужності роботи блоку. Бібл. 26, табл. 6, рис. 15.

Ключові слова: **пряме управління потужністю, управління з нечіткою логікою, синхронний генератор з постійними магнітами, метод ШІМ, вітроенергетична система.**

Introduction. The readily available renewable energy especially the abundant resources of solar energy and wind energy have led to a steady growth of interest concerning distributed generation units. As the adoption of system into the smart power grid is seen a tendency of becoming a new paradigm to sustainable energy, the integration of power converters to take control of the smart grid operation become one of the main research areas that require immense attention. The three phase grid connected voltage source converter which features Bidirectional power flow, nearly sinusoidal input currents, controllable power factor, and high quality DC output voltage have made it an increasingly important proportion in renewable energy system [1].

There are three type of renewable energy:

- mechanical energy (wind energy);
- electric energy (photovoltaic panels);
- energy in the form of heat (geothermal, solar [2]).

Wind energy, is one of the available non-conventional energy sources, which is clean and an infinite natural resource. Wind power is still the most promising renewable energy in the year of 2013. The wind turbine system (WTS) started with a few tens of kilowatt power in the 1980s. Now multi-megawatt wind turbines are widely installed even up to 6-8 MW [3] (Fig. 1).

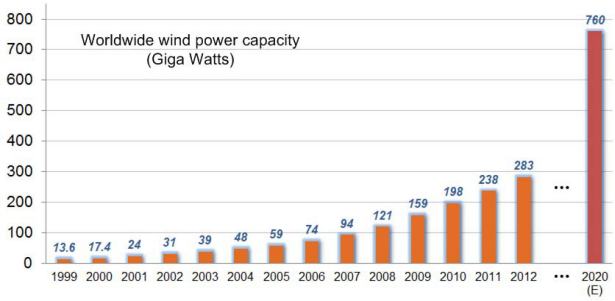

Fig. 1. Global cumulative installed wind power capacity from 1999 to 2020 [3]

Wind energy based power system operation is challenging under fluctuating nature of wind speeds and variable load conditions, particularly when the operation mode of the hybrid wind power system is stand alone. The changing wind speeds causes fluctuations in wind-turbine generator, which causes fluctuations in load

voltage and frequency in the stand-alone wind-energy system. Variable speed wind-turbine systems are more advantageous when compared with the fixed speed wind turbine systems. They generate maximum amount of power and gives less mechanical stress, higher power quality and efficiency than fixed speed wind-turbine systems [4, 5]. Standalone wind energy conversion systems are electric energy alternative sources for isolated area. They usually supplies air conditioning mechanical loads, ventilation and water pumps [6]. Various control strategies have been proposed in recent works on this type of PWM rectifier. It can be classified for its use of current rent loop controllers or active/reactive power controllers. The well-known method of indirect active and reactive power control is based on current vector orientation with respect to the line voltage vector. It is called voltage oriented control (VOC) [7]. VOC guarantees high dynamics and static performance via internal current control loops. However, the final configuration and performance of the VOC system largely depends on the quality of the applied current control strategy. Over the last few years, an interesting emerging control technique has been direct power control (DPC), developed analogously with the well-known direct torque control (DTC) used for adjustable speed drives [8].Therefore, the wind generating system is found to be of a great potential as a very attractive supply option for industrial and domestic applications. Several electrical generators can be used to perform the electromechanical energy conversion. Permanent magnet synchronous generator (PMSG) offer significant advantages over conventional synchronous generators as a source of isolated supply. Brushless, absence of a separate DC source, and maintenance free are among the advantages. However the variable natural of wind and the fluctuation of load profiles lead to fluctuating torque of the wind turbine generator. This causes variation in the output voltage and frequency [9]. The relay control can be performed by selecting an optimum switching state of the converter, so that the active and reactive power errors can be restricted in appropriate hysteresis bands, which is possible by using a switching table and several hysteresis comparators. The latter is based on a calculation of the voltages for each switching state of the converter by detecting the line currents, and the calculation is performed by utilizing the active and reactive power as intermediate variables. Since this method deals with instantaneous variables in obtaining the voltages, it is possible to estimate not only a fundamental component [10]. Fuzzy logic control has found many applications in the past two decades. This is so largely increasing because fuzzy logic control has the capability to control nonlinear uncertain systems even in the case where no mathematical model is available for the control system [11]. This paper proposes a novel DPC for a three phase PWM rectifier, which makes it possible to achieve unity power factor operation by directly controlling its instantaneous active and reactive power without any power-source voltage sensors. In this situation, the DPC based on fuzzy logic control is used instead of DPC. This control technique greatly lowers the fluctuations of the active and reactive power and the harmonic distortion rate THD [12].

This paper is organized into the following sections:

- Section I describes about the stand-alone wind energy system configuration with PMSG modeling;
- Section II represented different control strategies;
- Section III discusses about the simulation results;
- Conclusions.

Section I. Stand-alone wind energy supply system. The system consists of the following components (parameters are presented in Appendix in Tables A.1 – A.3):

- wind turbine;
- PMSG which is directly driven by the wind turbine without using a gearbox;
- uncontrolled rectifier PWM.

Profile wind turbine model. The first step necessary for a wind production project is the geographical choice of the site. The properties of wind are interesting for the study of the whole wind energy conversion system, since its power, under ideal conditions, is proportional to the cube of the wind speed. To know the characteristics of a site, it is essential to have measurements of the wind speed and its direction, over a long period of time. It is modeled by an addition of a number of harmonics and the wind speed variation is according to the following equation [13, 14]:

$$V = 6.5 + (0.2\sin(0.1074t) + 2\sin(0.2665t) + \sin(1.2930t) + \\ + 0.2\sin(3.6645t)). \quad (1)$$

Turbine modeling. The turbine is a device used to convert wind energy into mechanical energy. The mechanical power P of wind turbine extracted from the wind can be expressed as follows [15]

$$P = C_P P_\omega = \frac{1}{2} C_P \rho \pi R^2 V^3 , \quad (2)$$

where C_P is the power coefficient which is a function of the pitch angle of rotor blades θ [deg] and of the tip-speed ratio λ; P_ω is the dynamic force; ρ [kg/m^3] is the air density; R [m] is the blade turbine radius; V [m/s] is the wind speed.

The dynamic force accessible:

$$P_\omega = \frac{1}{2} \rho S V^3 = \frac{1}{2} \rho \pi R^2 V^3 . \quad (3)$$

The tip-speed ratio λ is defined as

$$\lambda = \frac{\Omega R}{V} , \quad (4)$$

where Ω is the angular mechanical speed of the turbine rotor.

Modeling of PMSG. AC machines are generally modeled by non-linear equations (differential equation). This non-linearity is due to the inductances and coefficients of the dynamic equations which depend on the rotor position and time. A three phase – two phase transformation necessary to simplify the model (reduce the number of equations). In the PMSG, the rotor excitation is supposed constant. The electrical equation represented by [16, 17]:

$$V_d = -R_s I_d - L_d \frac{d}{dt} I_d + \omega_r L_q I_q ; \quad (5)$$

$$V_q = -R_s I_q - L_q \frac{d}{dt} I_q - \omega_r L_d I_d + \omega_r \varphi_f , \quad (6)$$

where V_d and V_q are the components of stator voltage; R_s is the stator resistance; L_d and L_q are the components of stator inductances; I_d and I_q are the components of stator current; φ_f is the permanent magnet flux; ω_r is the electric pulsation; n_p is the pole pair number.

The electrical rotation speed is given by:

$$w_e = n_p \cdot w , \quad (7)$$

where n_p is the pole pair number; w is the mechanical speed.

The electromagnetic torque T_e represented by:

$$T_e = \frac{3}{2} \cdot n_p \cdot \varphi_f \cdot I_q . \quad (8)$$

The equations for active power P and reactive power Q are provided by:

$$P = \frac{3}{2}(V_d \cdot I_d - V_q \cdot I_q) ; \quad (9)$$

$$Q = \frac{3}{2}(V_q \cdot I_d - V_d \cdot I_q) . \quad (10)$$

Uncontrolled rectifier PWM. The wind generator, which is based on a variable speed turbine and a PMSG, is connected to a DC bus by through a PWM power converter [18]. Since we have three phase line voltage and the fundamental line currents in:

$$U_a = E_m \cos \omega t ; \quad (11)$$

$$U_b = E_m \cos(\omega t + \frac{2\pi}{3}) ; \quad (12)$$

$$U_c = E_m \cos(\omega t - \frac{2\pi}{3}) ; \quad (13)$$

$$i_a = I_m \cos(\omega t + \varphi) ; \quad (14)$$

$$i_b = I_m \cos(\omega t + \frac{2\pi}{3} + \varphi) ; \quad (15)$$

$$i_c = I_m \cos(\omega t - \frac{2\pi}{3} + \varphi) , \quad (16)$$

where E_m, I_m are the amplitudes of the phase voltage and current respectively; ω is angular frequency; φ is the phase shift.

Line to line input voltages of PWM rectifier can be described as:

$$U_{sa} = (s_a - s_b) \cdot u_{dc} ; \quad (17)$$

$$U_{sb} = (s_b - s_c) \cdot u_{dc} ; \quad (18)$$

$$U_{sc} = (s_c - s_a) \cdot u_{dc} , \quad (19)$$

and phase voltages equations give by:

$$U_{sa} = \frac{2s_a - (s_b + s_c)}{3} \cdot u_{dc} ; \quad (20)$$

$$U_{sb} = \frac{2s_b - (s_a + s_c)}{3} \cdot u_{dc} ; \quad (21)$$

$$U_{sc} = \frac{2s_c - (s_a + s_b)}{3} \cdot u_{dc} , \quad (22)$$

where s_a, s_b and s_c are the switching states of the rectifier and u_{dc} is voltage rectifier.

Section II. Generalized strategies control.

DPC of PMSG. The objective of the proposed command is to control the DC voltage at the input of the inverter u_{dc}. From the desired value of the DC voltage, it is possible to express that of the reference power by:

$$P_{ref} = u_{dc} \cdot i_{dc} , \quad (23)$$

where i_{dc} is the rectifier output current.

The principle of DPC and it was later developed for several applications. The aim was to eliminate the modulation block and the internal loops by replacing them with a switching table whose inputs are the errors between the reference values and the measurements. Then, a similar technique was proposed for a rectifier control application (generator in our case). In this case, the quantities controlled are the instantaneous active and reactive powers, use this quantity as control variables and which does not need to use modulation blocks because the switching because the switching states are chosen directly by a switching table .

Figure 2 gives the DPC structure adopted for the application studied.

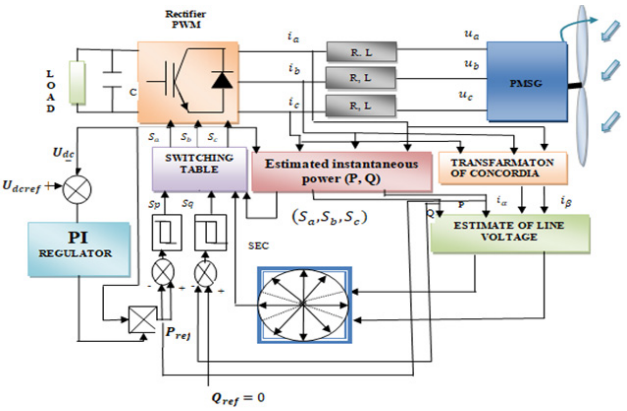

Fig. 2. Diagram of DPC for the PMSG

Estimated instantaneous power. The instantaneous active power is defined by the dot product between the currents and the line voltages. Whereas, the reactive power is defined by the vector product between them [19, 20]:

$$\overline{S} = \overline{U} \times \overline{I} = P + jQ ; \quad (24)$$

$$\overline{S} = U_a \cdot i_a + U_b \cdot i_b + U_c \cdot i_c + j\frac{1}{\sqrt{3}}[(U_b - U_c)i_a + (U_C - U_a)i_b + (U_a - U_b)i_c], \quad (25)$$

where U is instantaneous source voltage; I: is line instantaneous current; L is the line inductance

$$Q = \frac{1}{\sqrt{3}}[3L(\frac{di_a}{dt} i_c + \frac{d_{ic}}{dt} i_a) - u_{dc}(S_a(i_b - i_c) + S_b(i_c - i_a) + S_c(i_a - i_b))]; \quad (26)$$

$$P = L(\frac{di_a}{dt} i_a + \frac{di_b}{dt} i_b + \frac{di_c}{dt} i_c) + u_{dc}(S_a i_a + S_b i_b + S_c i_c). \quad (27)$$

The first parts of the two expressions represented above present the power in the line inductors, noting here that the internal resistances of these inductors are negligible because the active power dissipated in these resistors is in fact much lower compared to the power involved. Other parts represent the power in the converter.

Voltage estimation. The line voltage working area is required to determine the switching orders. In addition it is important to estimate the line voltage correctly, even with the existence of harmonics, its gives a high power

factor. The following expression gives the line currents i_a, i_b, i_c in the stationary coordinates $\alpha - \beta$

$$\begin{bmatrix} i_\alpha \\ i_\beta \end{bmatrix} = \sqrt{\frac{2}{3}} \begin{bmatrix} 1 & \frac{-1}{2} & \frac{-1}{2} \\ 0 & \frac{\sqrt{3}}{2} & \frac{-\sqrt{3}}{2} \end{bmatrix} \begin{bmatrix} i_a \\ i_b \\ i_c \end{bmatrix}. \quad (28)$$

We can write the expressions of the active and reactive powers as follows [21]:

$$P = \underline{V}_{(abc)} \cdot i_{(abc)} = \underline{V_\alpha} \underline{i_\alpha} + \underline{V_\beta} \underline{i_\beta}; \quad (29)$$

$$Q = \underline{V}_{(abc)} \wedge i_{(abc)} = \underline{V_\alpha} \underline{i_\beta} - \underline{V_\beta} \underline{i_\alpha}. \quad (30)$$

The matrix writing of the expressions (29) and (30) is:

$$\begin{bmatrix} P \\ Q \end{bmatrix} = \begin{bmatrix} V_\alpha & V_\beta \\ -V_\alpha & V_\alpha \end{bmatrix} \begin{bmatrix} i_\alpha \\ i_\beta \end{bmatrix}. \quad (31)$$

The matrix equation (31) can be rewritten, depending on the line current (measured) and the power (estimated), as follows:

$$\begin{bmatrix} V_\alpha \\ V_\beta \end{bmatrix} = \frac{1}{i_\alpha^2 + i^2 \beta} \begin{bmatrix} i_\alpha & -i_\beta \\ i_\beta & i_\alpha \end{bmatrix} \begin{bmatrix} P \\ Q \end{bmatrix}. \quad (32)$$

Concordia's inverse transform of line voltages is written [22]:

$$\begin{bmatrix} V_a \\ V_b \\ V_c \end{bmatrix} = \sqrt{\frac{2}{3}} \begin{bmatrix} 1 & 0 \\ \frac{-1}{2} & \frac{\sqrt{3}}{2} \\ \frac{-1}{2} & \frac{-\sqrt{3}}{2} \end{bmatrix} \begin{bmatrix} V_\alpha \\ V_\beta \end{bmatrix}. \quad (33)$$

Hysteresis controller. The main idea behind the DPC method is to maintain the instantaneous active and reactive powers within a desired band. DPC consists of two hysteresis comparators whose inputs are the errors between the reference and estimated values of the active and reactive powers, respectively.

$$\begin{cases} \Delta P = P_{ref} - P; \\ \Delta Q = Q_{ref} - Q. \end{cases} \quad (33)$$

The hysteresis comparators provide two logic outputs d_P and d_Q. The state «1» corresponds to an increase in the controlled variable (P and Q), while «0» corresponds to a decrease

$$\begin{cases} if \Delta P \geq h_p \Rightarrow d_p = 1; \\ if \Delta P \prec -h_P \Rightarrow d_P = 0; \\ if \Delta Q \geq h_Q \Rightarrow d_Q = 1; \\ if \Delta Q \prec -h_Q \Rightarrow d_Q = 0, \end{cases} \quad (35)$$

where h_P and h_Q denote the hysteresis bands [21].

Switching table. The digital error signals S_P and S_Q and the working sector are the inputs of the switching table where the switching states S_a, S_b and S_c the PWM rectifier are stored. By using the table, the optimum switching state Of the converter can be chosen at each switching state according to the combination of the digital signals S_P and S_Q sector number, that is to say, that the choice of the optimum switching state is made so that the error of the active power can be restricted in a hysteresis band of width 2H_p, and likewise for the error of reactive power, with a band of width [22].

The sectors can be numerically expressed as:

$$(n-2)\frac{\pi}{6} \leq \theta_n \leq (n-1)\frac{\pi}{6}), \quad (36)$$

where n = 1, 2, ... ,12.

By using several comparators, it is possible to specify the sector where the voltage vector exists. The digitized error signals S_P and S_Q digitized voltage phase are θ_n input to the switching table in which every switching state of the converter is stored, as shown in Table 1. By using this switching table, the optimum switching state S_a, S_b and S_c of the converter can be selected uniquely in every specific moment according to the combination of the digitized input signals (Fig. 3). The selection of the optimum switching state is performed so that the power errors can be restricted within the hysteresis bands [23].

Table 1

Possible switching table

S_P	S_Q	θ_1	θ_2	θ_3	θ_4	θ_5	θ_6
0	0	v_6	v_1	v_1	v_2	v_2	v_3
	1	v_1	v_2	v_2	v_3	v_3	v_4
1	0	v_5	v_6	v_6	v_1	v_1	v_2
	1	v_3	v_4	v_4	v_5	v_5	v_6
S_P	S_Q	θ_7	θ_8	θ_9	θ_{10}	θ_{11}	θ_{12}
0	0	v_3	v_4	v_4	v_5	v_5	v_6
	1	v_4	v_5	v_5	v_6	v_6	v_1
1	0	v_2	v_3	v_3	v_4	v_4	v_5
	1	v_6	v_1	v_1	v_2	v_2	v_3

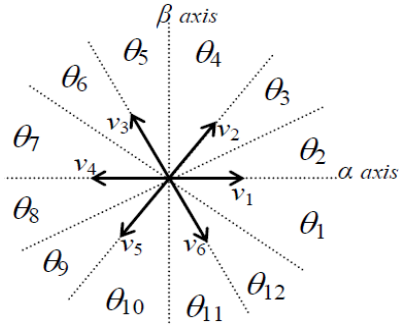

Fig. 3. The vector plane divided into 12 sectors

External voltage regulation loop. The external regulation loop maintains a load assimilated to a resistance R. The impedance thus formed is charged by the current i_{dc} from the PWM rectifier. The current i_{dcref} is the current from the PWM rectifier (Fig. 4). The product of the reference DC with the DC voltage gives the active power of reference. Capacitance voltage DC at a reference voltage is u_{dcref}. The capacity C is in parallel with load (resistance).

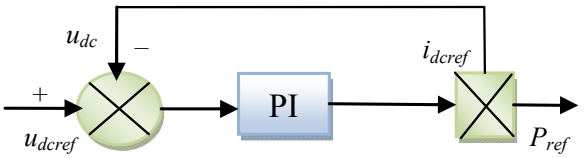

Fig. 4. DC voltage regulation

Fuzzy logic control for DPC. Improving the quality of the currents absorbed by the PWM rectifier and maintaining of the DC voltage at the output around the of the DC voltage at the output around the reference requires voltage regulation and fast and robust currents[24]. For this reason presents a DPC operating with a fuzzy logic controller which replaces voltage in conventional commands. Figure 5 gives the block diagram of the proposed fuzzy logic controller for DPC of three-phase PWM rectifier.

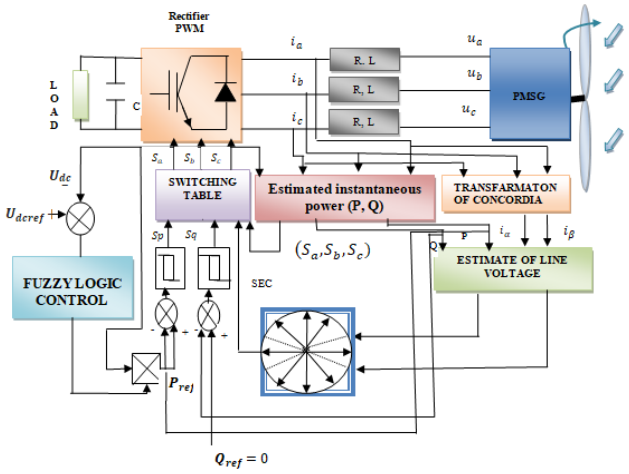

Fig. 5.The block diagram e block diagram of fuzzy logic controller for DPC of three-phase PWM rectifier

The configuration of the voltage loop is illustrated in Fig. 6, it is composed of [25]:

- normalization factors relate to the error (e) and the variation of the command (Δe);
- a block of fuzzyfication of the error and its variation;
- rule of inference. The control strategy is presented by an inference matrix presented in table;
- a defuzzification block used to convert the fuzzy control variation into a digital value.

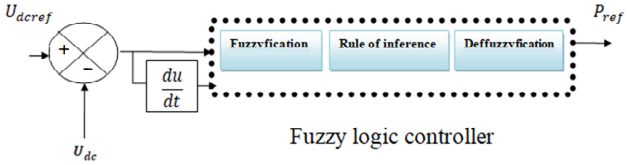

Fig. 6. Diagram of the proposed fuzzy logic controller for DPC

Fuzzyfication. This step deals with the transformation of numeric values to inputs into fuzzy values or linguistic variables. The input variables which are the velocity error and its variation are subjected to a fuzzification operation and therefore converted to fuzzy sets. The normalized universe of speech of each variable of the regulator (the error, its variation and the variation of variation and the variation of the command) is subdivided into seven fuzzy sets; these are characterized by the following standard designations:

- large negative noted LN;
- average negative noted AN;
- small negative noted SN;
- about zero noted AZ;
- positive small noted PS;
- average positive noted AP;
- large positive noted LP.

For the membership functions we chose for each variable the triangular and trapezoidal shapes**.**

Inference rules. The rule base represents the control strategy and desired goal through linguistic control rules. It makes it possible to determine the decision or action at the output of the fuzzy controller and to express qualitatively the relationship that exists between the input variables and the output variable. From the study of the behavior of the system, we can establish the control rules, which connect the output with the inputs. As we mentioned, each of the two linguistic inputs of the fuzzy controller has seven fuzzy sets.

Fuzzy rules table (Table 2) showing change in control output [26].

Table 2

Fuzzy rules table

e / Δe	LN	AN	SN	AZ	PS	AP	LP
LN	LN	LN	LN	LN	AN	SN	AZ
AN	LN	LN	LN	AN	SN	AZ	PS
SN	LN	LN	AN	SN	AZ	PS	AP
AZ	LN	AN	SN	AZ	PS	AP	LP
PS	AN	SN	AZ	PS	AP	LP	LP
AP	SN	AZ	PS	AP	LP	LP	LP
LP	AZ	PS	AP	LP	LP	LP	LP

The logic for determining this matrix of rules is based on a global or qualitative knowledge of the functioning of the system. As an example, consider the following two rules:

- if e is LP and Δe is LP then Δu is LP;
- if e is AZ and Δe is AZ then Δu is AZ.

They indicate that if the speed is too small compared to its reference (e is LP and Δe is LP), then a large torque demand (Δu is PG) is needed (to bring the speed back to its reference). And if the speed meets its reference and settles (e is AZ and Δe is AZ) then keep the same torque (Δu is EZ).

Deffuzzyfication. When the fuzzy output is calculated, it must be transformed into a numeric value. There are several methods to achieve this transformation. The most used is the center of gravity method, which we have adopted in our work. The abscissa of the center of gravity corresponding to the output of the regulator is given by:

$$\Delta U = \frac{\int x\gamma(x)dx}{\int \gamma(x)dx}. \qquad (37)$$

Section III. Discusses about the simulation results and discussion. Simulations and results of DPC are presented in Fig. 7-15. We present the wind turbine profile (Fig. 7); the stator voltages of PMSG (Fig. 8); the stator voltage and current of PMSG (Fig. 9); the rectified

voltage DPC (Fig. 10); the active (Fig. 11) and reactive Fig. 12) power for classic DPC and fuzzy DPC technique (Fig. 13-15).

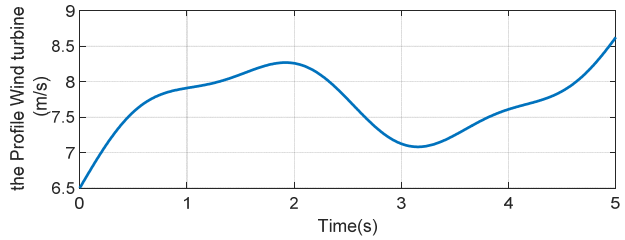

Fig. 7. The profile wind turbine

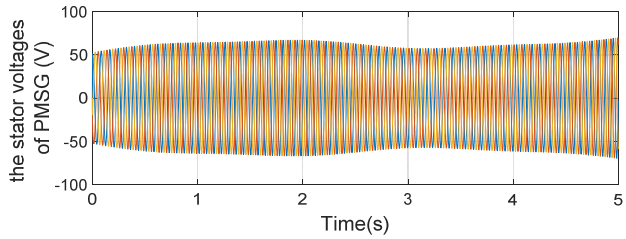

Fig. 8.The stator voltages of PMSG

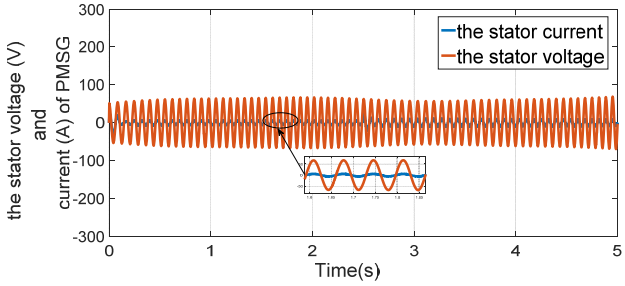

Fig. 9. The stator voltage and current of PMSG

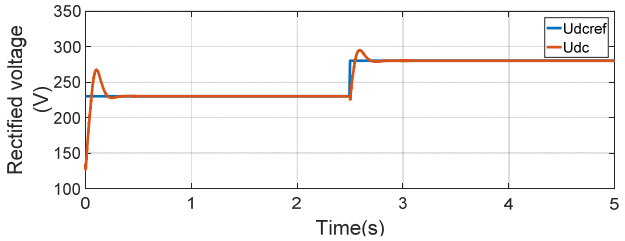

Fig. 10. The rectified voltage DPC

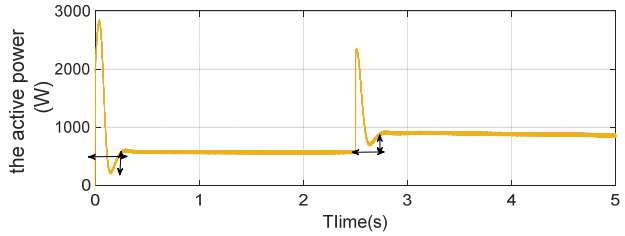

Fig. 11. The active power DPC

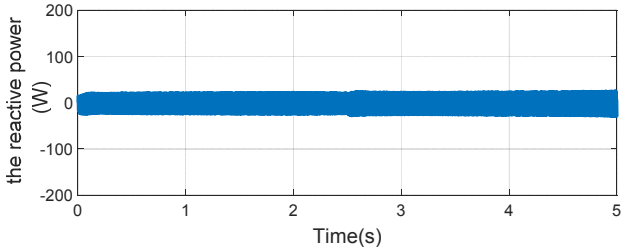

Fig. 12. The reactive power DPC

Simulations and results of Fuzzy logic control for DPC.

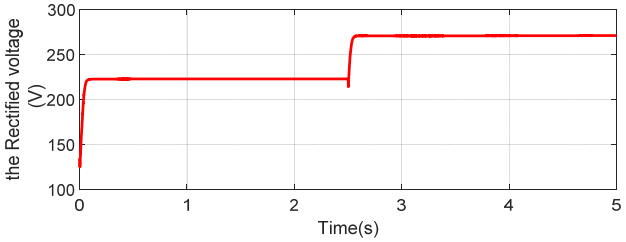

Fig. 13. Rectified voltage DPC fuzzy logic

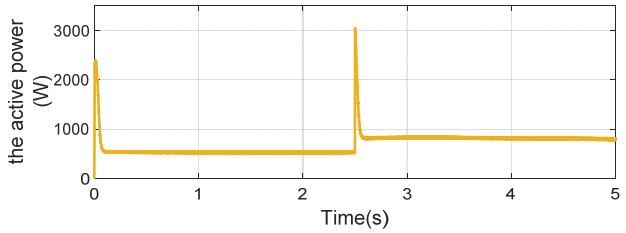

Fig. 14. The active power DPC fuzzy logic

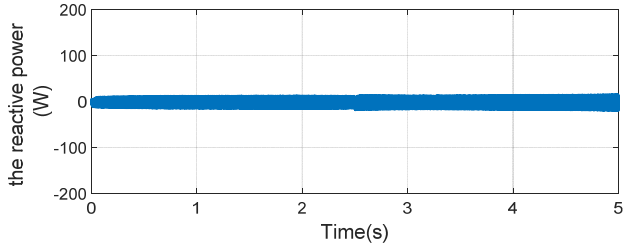

Fig. 15. The reactive power DPC fuzzy logic

During the transient response (Fig. 10) shows that there is an overshooting in the rectifier output voltage caused by PI parameters choice and the signal produced by the start of the PMSG, but at (t = 0.3 to 2.5 s), note that the direct voltage reaches its reference value (230 V) and (280 V), but for fuzzy logic the direct voltage reaches its reference value from (t =0 to 0.025 s) (Fig. 13), and the instantaneous powers (P, Q) followed by the reference power (P = 550 W) and (P =850 W) in the Fig. 11, and (q = 0 vAR) with a considerable presence of oscillations around the reference (Fig. 12), but for the DPC by PI regulator from (t = 0 to 0.3 s) the response very slow and from (t = 2.5 to 2.8 s) it there is a disturbance produced by the change of the reference voltage on the other hand fuzzy logic DPC instantaneous powers (P, Q) followed by the reference power from (t = 0.24 s) and response time speed very and the absence of disturbance produced by the change in the reference voltage (Fig. 14) and decrease in oscillations around the reference (Fig. 15), the voltage and current of the PMSG are in phase, and the line currents are sinusoidal (Fig. 9).

The active and reactive power responses follow their references perfectly, these results, show the superiority of fuzzy regulator compared to the conventional PI. With fuzzy regulators no overshoot is produced, fast response in transient conditions and the static error is nearly zero.

THD comparative study. The objective of this study is to show the contribution of each two methods presented throughout this work. The two criteria taken into account in evaluating the performance of these

controls are: the rate of distortion of the network currents (THD). Table 3 shows the THD values obtained in steady state for the two control modes. All of these commands give acceptable THD values of less than 5 %. We also notice the superiority of fuzzy logic regulator over the other control; in fact, it can reduce the THD to a low value of approximately 1.87 %.

Table 3

THD values

Control	Classical regulator PI for DPC	Fuzzy logic control for DPC
THD % (f = 12.8 Hz)	3.58 %	1.87 %

Conclusion.

The proposed control is simple, robust, not sensitive to the parametric disturbance and variation of the system, and with very good dynamic characteristics. For DPC fuzzy the value of rectified voltage is 0.025 s and very speed time response of disturbance produced by the change in the reference voltage 0.01 s. It can be said that the use of fixed PI regulators gives a robust control system and an acceptable response 0.3 s, but the conventional problems of the PI regulator such as the response time and the robustness against external disturbances have appeared, and to solve the problems mentioned above we will use the fuzzy control to establish a regulator robust.

The fuzzy logic adjustment gives a very programmatic approaches, allowing integrating the knowledge acquired by the operators.

Spectral analysis of line current shows that all low-order harmonics are well attenuated which gives a THD around to 3.6 %.

The fuzzy DPC simulation results obtained good performance in steady state and transient conditions especially for the case of current harmonic distortion rate which is good for other techniques; it is able to reduce the THD to a low value of around 1.87 % with better convergence of active power (P = 550 W and P =850 W), however reactive power (q = 0 vAR) towards their respective references.

APPENDIX

Table A.1

Wind turbine parameters

Parameter	Symbol	Value
Power	P	7.5 kW
Radius	R	3.24 m
Inertia	J	7.5 kg·m^2
Friction coefficient	F	0.06 N·m·s/rad

Table A.2

PMSG parameters

Parameter	Symbol	Value
Direct stator inductance	L_d	0.012 H
Stator quadrature inductance	L_q	0.0211 H
Permanent magnet flux	φ_f	0.9 Wb
Stator resistance	R_S	0.895 Ω
Inertia	J	0.00141 kg·m^2
Number of poles	n_p	3
Friction force	F	0 N·m/rad·s

Table A.3

Rectifier parameters

Parameter	Symbol	Value
Line resistance	R_l	0.7 Ω
Line inductance	L	0.01 H
Filtering capacity	C	0.0033 F
DC voltage reference	U_{dcref}	230 – 280 V

REFERENCES

1. Rodriguez J.R., Dixon J.W., Espinoza J.R., Pontt J., Lezana P. PWM regenerative rectifiers: state of the art. *IEEE Transactions on Industrial Electronics*, 2005, vol. 52, no. 1, pp. 5-22. **doi: 10.1109/TIE.2004.841149.**

2. Singh M., Chandra A., Singh B. Sensorless Power maximization of PMSG based isolated wind-battery hybrid system using adaptive neuro-fuzzy controller. *2010 IEEE Industry Applications Society Annual Meeting*, Oct. 2010. **doi: 10.1109/IAS.2010.5615370.**

3. Blaabjerg F., Ke Ma. Future on power electronics for wind turbine systems. *IEEE Journal of Emerging and Selected Topics in Power Electronics*, 2013, vol. 1, no. 3, pp. 139-152. **doi: 10.1109/JESTPE.2013.2275978.**

4. Barton J.P., Infield D.G. Energy storage and its use with intermittent renewable energy. *IEEE Transactions on Energy Conversion*, 2004, vol. 19, no. 2, pp. 441-448. **doi: 10.1109/TEC.2003.822305.**

5. Barote L., Marinescu C., Cirstea M.N. Control structure for single-phase stand-alone wind-based energy sources. *IEEE Transactions on Industrial Electronics*, 2013, vol. 60, no. 2, pp. 764-772. **doi: 10.1109/TIE.2012.2206346.**

6. Badran O. Wind turbine utilization for water pumping in Jordan. *Journal of Wind Engineering and Industrial Aerodynamics*, 2003, vol. 91, no. 10, pp. 1203-1214. **doi: 10.1016/S0167-6105(03)00073-4.**

7. Malinowski M., Kazmierkowski M.P., Trzynadlowski A. Review and comparative study of control techniques for three-phase PWM rectifiers. *Mathematics and Computers in Simulation*, 2003, vol. 63, no. 3-5, pp. 349-361. **doi: 10.1016/S0378-4754(03)00081-8**.

8. Larrinaga S.A., Vidal M. A. R., Oyarbide E., Apraiz J. R. T. Predictive control strategy for DC/AC converters based on direct power control. *IEEE Transactions on Industrial Electronics*, 2007, vol. 54, no. 3, pp. 1261-1271. **doi: 10.1109/TIE.2007.893162**.

9. Mendis N., Muttaqi K.M., Perera S. Management of battery-supercapacitor hybrid energy storage and synchronous condenser for isolated operation of PMSG based variable-speed wind turbine generating systems. *IEEE Transactions on Smart Grid*, 2014, vol. 5, no. 2, pp. 944-953. **doi: 10.1109/TSG.2013.2287874.**

10. Noguchi T., Tomiki H., Kondo S., Takahashi I., Katsumata J. Instantaneous active and reactive power control of PWM converter by using switching table. *IEEJ Transactions on Industry Applications*, 1996, vol. 116, no. 2, pp. 222-223. **doi: 10.1541/ieejias.116.222.**

11. Idir A., Kidouche M. Direct torque control of three phase induction motor drive using fuzzy logic controllers for low torque ripple. *Proceedings Engineering & Technology*, 2013, vol. 2, pp. 78-83.

12. Boukhechem I., Boukadoum A., Boukelkoul L., Lebied R. Sensorless direct power control for three-phase grid side converter integrated into wind turbine system under disturbed grid voltages. *Electrical engineering & electromechanics*, 2020, no. 3, pp. 48-57. **doi: 10.20998/2074-272X.2020.3.08.**

13. Mirecki A., Roboam X., Richardeau F. Architecture complexity and energy efficiency of small wind turbines. *IEEE Transactions on Industrial Electronics*, 2007, vol. 54, no. 1, pp. 660-670. **doi: 10.1109/tie.2006.885456.**

14. Tran D.-H., Sareni B., Roboam X., Espanet C. Integrated optimal design of a passive wind turbine system: an experimental validation. *IEEE Transactions on Sustainable Energy*, 2010, vol. 1, no. 1, pp. 48-56. **doi: 10.1109/tste.2010.2046685.**

15. Cho Y., Lee K.-B., Song J.-H., Lee Y.I. Torque-ripple minimization and fast dynamic scheme for torque predictive control of permanent-magnet synchronous motors. *IEEE Transactions on Power Electronics*, 2015, vol. 30, no. 4, pp. 2182-2190. **doi: 10.1109/TPEL.2014.2326192.**

16. Chinchilla M., Arnaltes S., Burgos J.C. Control of permanent-magnet generators applied to variable-speed wind-energy systems connected to the grid. *IEEE Transactions on Energy Conversion*, 2006, vol. 21, no. 1, pp. 130-135. **doi: 10.1109/TEC.2005.853735.**

17. Kim H.-W., Kim S.-S., Ko H.-S. Modeling and control of PMSG-based variable-speed wind turbine. *Electric Power Systems Research*, 2010, vol. 80, no. 1, pp. 46-52. **doi: 10.1016/j.epsr.2009.08.003.**

18. Seyoum D., Rahman M.F., Grantham C. Terminal voltage control of a wind turbine driven isolated induction generator using stator oriented field control. *Eighteenth Annual IEEE Applied Power Electronics Conference and Exposition*, 2003. APEC '03. **doi: 10.1109/APEC.2003.1179315.**

19. Bouafia A., Gaubert J.-P., Krim F. Predictive direct power control of three-phase pulsewidth modulation (PWM) rectifier using space-vector modulation (SvM). *IEEE Transactions on Power Electronics*, 2010, vol. 25, no. 1, pp. 228-236. **doi: 10.1109/TPEL.2009.2028731.**

20. Malinowski M., Kazmierkowski M.P., Trzynadlowski A. Review and comparative study of control techniques for three-phase PWM rectifiers. *Mathematics and Computers in Simulation*, 2003, vol. 63, no. 3-5, pp. 349-361. **doi: 10.1016/S0378-4754(03)00081-8.**

21. Bouafia A., Gaubert J.-P., Krim F. Analysis and design of new switching table for direct power control of three-phase PWM rectifier. *2008 13th International Power Electronics and Motion Control Conference*, Sep. 2008. **doi: 10.1109/epepemc.2008.4635347.**

22. Hussein M.M., Senjyu T., Orabi M., Wahab M.A.A., Hamada M.M. Load power management control for a stand alone wind energy system based on the state of charge of the battery. *2012 IEEE International Conference on Power and Energy (PECon)*, Dec. 2012. **doi: 10.1109/pecon.2012.6450352.**

23. Noguchi T., Tomiki H., Kondo S., Takahashi I. Direct power control of PWM converter without power-source voltage sensors. *IEEE Transactions on Industry Applications*, 1998, vol. 34, no. 3, pp. 473-479. **doi: 10.1109/28.673716.**

24. Ohnuki T., Miyashita O., Lataire P., Maggetto G. Control of a three-phase PWM rectifier using estimated AC-side and DC-side voltages. *IEEE Transactions on Power Electronics*, 1999, vol. 14, no. 2, pp. 222-226. **doi: 10.1109/63.750174.**

25. Benbouhenni H., Boudjema Z. Comparative study between neural hysteresis, fuzzy PI, and neural switching table for an IM DTC control. *Proceedings of the World Congress on Engineering and Computer Science*, 2018, vol. 5.

26. Bouafia A., Krim F., Gaubert J.-P. Design and implementation of high performance direct power control of three-phase PWM rectifier, via fuzzy and PI controller for output voltage regulation. *Energy Conversion and Management*, 2009, vol. 50, no. 1, pp. 6-13. **doi: 10.1016/j.enconman.2008.09.011.**

Received 05.09.2020
Accepted 19.10.2020
Published 24.12.2020

Ryma Lebied [1]*, Ph.D.,*
Rachid Lalalou[1]*, Doctor of Electrotechnical,*
Hocine Benalla[2]*, Doctor of Electrotechnical, Professor,*
Khalil Nebti[2]*, Doctor of Electrotechnical,*
Ismail Boukhechem[1]*, Ph.D.,*
[1] Electrotechnical Laboratory Skikda (LES),
University 20 August 1955,
Department of Electrical Engineering,
26 Road El Hadaiek 21000, Skikda, Algeria.
[2] Electrical Engineering Laboratory of Constantine, LEC,
Department of Electrical Engineering,
University of Constantine 1, 25000 Constantine, Algeria.
e-mail: r.lebied@univ-skikda.dz; rlalalou@yahoo.fr;
benalladz@yahoo.fr; idor2003@gmail.com;
sameu25@gmail.com